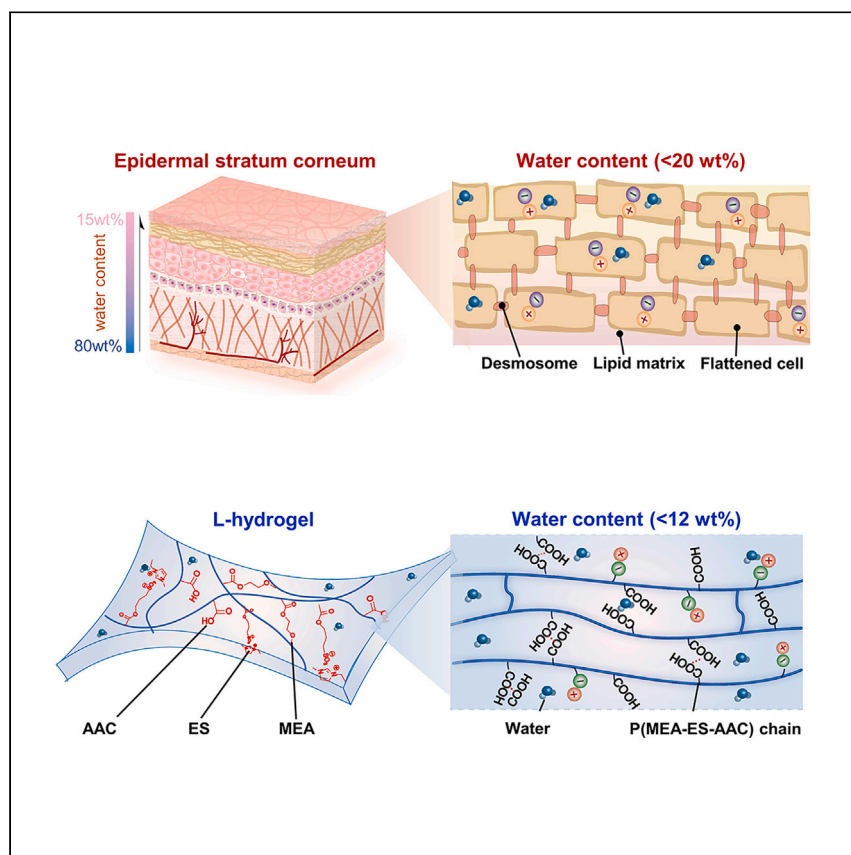


Article

Low-water-content polyelectrolyte hydrogels inspired by human epidermal stratum corneum



Inspired by the low/stable water content of human epidermis, Shen et al. report a low-water-content polyelectrolyte hydrogel (L-hydrogel) that mimics the composition of human epidermal stratum corneum employing an integrated hydrophobic/hydrophilic network design. L-hydrogels possess excellent mechanical properties and stability in air, enabling various soft ionotronics with long-lasting stable functionality.

Zihang Shen, Jie Ma, Yijie Cai, ..., Canhui Yang, Shaoxing Qu, Zheng Jia

zheng.jia@zju.edu.cn

Highlights

L-hydrogels possess extraordinary mechanical properties

L-hydrogels are mechanically and electrically stable in air

L-hydrogels enable soft ionotronics with long-term stability

Article

Low-water-content polyelectrolyte hydrogels inspired by human epidermal stratum corneum

Zihang Shen,¹ Jie Ma,¹ Yijie Cai,¹ Siyang Li,¹ Dongrui Ruan,¹ Shufen Dai,² Zhi Sheng,¹ Jiabao Bai,¹ Daochen Yin,¹ Jianfeng Ping,² Yibin Ying,² Canhui Yang,³ Shaoxing Qu,¹ and Zheng Jia^{1,4,*}

SUMMARY

Hydrogels typically contain large amounts of water (>80 wt %) and suffer from limitations inherent to high water content, including rapid dehydration under ambient conditions and limited mechanical properties. Herein, inspired by the low water content and stable performance of human epidermis, we report a low-water-content polyelectrolyte hydrogel (i.e., L-hydrogel) that mimics the composition of the human epidermal stratum corneum by employing an integrated hydrophobic/hydrophilic network design. The low water content of L-hydrogels (<12 wt %) leads to superior self-healing capability with a healing efficiency of ~100%, strength and modulus approaching ~1 MPa, skin-like fracture toughness (3,390 J/m²), and strong natural adhesions (~120–1,300 N/m) to both wet and dry surfaces. L-hydrogels also possess stable water content and mechanical properties over time under ambient conditions, enabling long-lasting stable functionality for various types of triboelectric nanogenerators and ionic skins. L-hydrogels hold promise for long-term practical applications in soft ionotronics under ambient conditions.

INTRODUCTION

Hydrogels are polymer networks containing large amounts of water (typically >80 wt %). With their excellent transparency,^{1,2} ionic conductivity,^{3–5} and widely tunable mechanical properties,^{6–8} hydrogels have been utilized in a wide range of applications, including biomedicine,^{9–11} flexible electronics,^{12,13} tissue engineering,^{14,15} and soft machines.^{16,17} However, ordinary hydrogels of high water content suffer from key limitations inherent to water, which tends to leak, evaporate, and interfere with interchain molecular interactions, causing a host of issues.^{18,19} First, due to the volatile nature of water, hydrogels are often plagued by rapid dehydration, as is commonly observed under ambient conditions, causing severe deterioration of the mechanical²⁰ and electrical properties²¹ of hydrogels. At temperatures below 0°C, the large amount of water in the hydrogel easily freezes, resulting in the loss of elasticity and functionality of the hydrogel.²² Methods such as hydrogel encapsulation^{23,24} and the introduction of organic solvents^{25,26} and salts²⁷ have been proposed to alleviate the dehydration and icing but cannot fundamentally avoid these issues, especially the water loss from hydrogels under ambient conditions. Secondly, the high content of water can compromise the mechanical properties of hydrogels, such as tensile strength,^{28,29} adhesion energies,³⁰ and self-healing capabilities.³¹ For example, the high water content weakens molecular interactions (e.g., hydrogen bonds) between the polymer chains of hydrogels, and as a result, the tensile strength of high-water-content hydrogels is usually below 100 kPa.²⁹ In addition, the abundance of water in a hydrogel poses a particular challenge to adhesion since water

¹State Key Laboratory of Fluid Power and Mechatronic Systems, Key Laboratory of Soft Machines and Smart Devices of Zhejiang Province, Center for X-Mechanics, Department of Engineering Mechanics, Zhejiang University, Hangzhou 310027, China

²Laboratory of Agricultural Information Intelligent Sensing, School of Biosystems Engineering and Food Science, Zhejiang University, Hangzhou 310058, China

³Shenzhen Key Laboratory of Soft Mechanics & Smart Manufacturing, Department of Mechanics and Aerospace Engineering, Southern University of Science and Technology, Shenzhen 518055, China

⁴Lead contact

*Correspondence: zheng.jia@zju.edu.cn
<https://doi.org/10.1016/j.xcrp.2023.101741>

molecules in a hydrogel change neighbors readily and transmit force negligibly. Without special adhesion treatment, a hydrogel often does not adhere strongly to any material, especially wet surfaces—the adhesion energy is usually on the level of 10 J/m^2 .³⁰ Last but not least, many existing conductive hydrogels are hydrogels containing dissolved salts. That is, both anions and cations in these hydrogels are able to move freely in the solvent, so they tend to leak as water migrates, resulting in a severe loss of conductivity.³² To this end, the prevention of water loss and ion leakage and the improvement of mechanical properties (especially strength and adhesion) of conventional hydrogels are essential for the practical applications of ionic conductors, which require long-term stability and excellent material properties of hydrogels.

Human epidermal stratum corneum—the outermost layer of the epidermis—consists of several layers of flattened cells linked by desmosomes and embedded in a lipid matrix, as illustrated in [Figure 1A](#). The water content of the stratum corneum is stable between 10 and 20 wt % throughout the year under ambient conditions,³³ endowing the human skin with long-term stability and sufficient mechanical strength under ambient conditions and even harsh environments,³⁴ thereby protecting people from dehydration and mechanical stress.³⁵ The stratum corneum of human epidermis is mainly comprised of proteins, lipids, and natural moisturizing factors (NMFs).³⁶ Among them, proteins in the flattened cell membrane and desmosomes play the role of coagulation and enhancement, imparting extraordinary mechanical strength and wound-healing capability to the human skin.³⁷ NMFs are principally hygroscopic amino acids encapsulated in human epidermal cells. The importance of an NMF lies in the strong hygroscopicity of its chemical components, especially pyrrolidone carboxylic acid and lactate,³⁸ which absorb moisture from the atmosphere and thus act as moisturizers for the skin. The NMF and proteins are hydrophilic, while lipids are hydrophobic. The moisture absorption of NMFs and the hydrophobic effect of lipids can maintain the water content of the skin at a relatively low level (usually below 20 wt %).³⁹ Moreover, dissociated ions of the hydrophilic amino acids of NMFs can conduct electricity and are difficult to leak due to the confinement effect of the epidermal cell membrane, conferring stable bioelectrical properties to the human stratum corneum.

Inspired by the composition of the human epidermal stratum corneum and the mechanical/electrical/hygroscopic functions of each composition, we develop a low-water-content polyelectrolyte hydrogel (L-hydrogel) by copolymerizing 1-ethyl-3-methyl imidazolium (3-sulfopropyl) acrylate (ES), acrylic acid (AAC), and methoxyethyl acrylate (MEA), which mimic the role of NMFs, proteins, and lipids, respectively ([Figure 1B](#)). The introduction of ES can also mimic the non-leakage properties of the ions of NMFs in the stratum corneum since the anions of ES are anchored to the polymer backbone of the hydrogel and can attract the dissociated cations via electrostatic forces, which makes the cations much less likely to leak compared to hydrogels containing dissolved salts. In stark contrast to traditional hydrogels of high water content ($>80 \text{ wt } \%$), the water content of the L-hydrogel under ambient conditions is below 12 wt %—similar to that of human stratum corneum—and can remain stable for long periods of time, which avoids deterioration of hydrogel properties due to water loss under ambient conditions and improves the stability of mechanical and electrical properties of the L-hydrogel. In addition, the low-water-content strategy results in L-hydrogels with excellent self-healing capabilities (self-healing efficiency of $\sim 100\%$), enhanced strength (0.98 MPa) and modulus (0.93 MPa), excellent fracture toughness comparable to human skin ($3,390 \text{ J/m}^2$), and strong natural adhesion ($\sim 120\text{--}1,300 \text{ N/m}$) to various wet and dry surfaces. Finally,

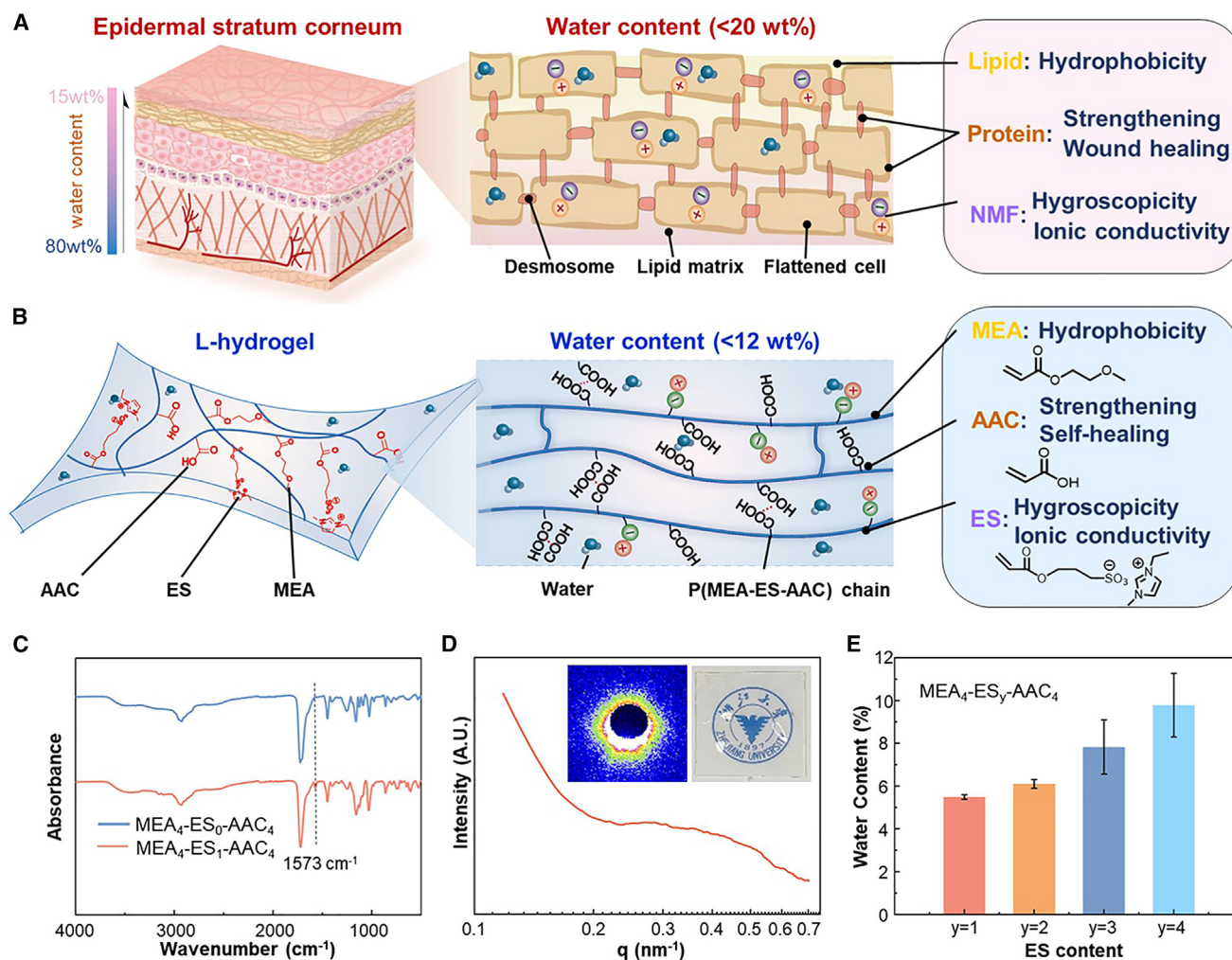


Figure 1. Molecular design and physical properties of L-hydrogels inspired by human epidermal stratum corneum

(A) Schematic diagram of the human epidermal stratum corneum. The stratum corneum is mainly comprised of proteins, lipids, and NMFs. Proteins present in desmosomes and cell membranes contribute to the mechanical strength and wound-healing capability of the human epidermis. The hygroscopic NMF with dissociated ions enables ionic conductivity and enhances moisture absorption. Lipids are hydrophobic, balancing the water content in the stratum corneum.

(B) Schematics of the L-hydrogel. The L-hydrogels are synthesized by copolymerizing 1-ethyl-3-methyl imidazolium (3-sulfopropyl) acrylate (ES), acrylic acid (AAC), and methoxyethyl acrylate (MEA), which mimic the role of NMFs, proteins, and lipids, respectively.

(C) The FTIR spectrum of the MEA₄-ES₁-AAC₄ L-hydrogels. The result indicates the successful polymerization of ES into the L-hydrogels.

(D) The SAXS profile of the L-hydrogels. Inset: a logo of Zhejiang University covered by a transparent L-hydrogel film.

(E) The water content of L-hydrogels with different ES content. All L-hydrogels contain water content of less than 12 wt % under ambient conditions. Error bars represent the standard deviation.

we realize the long-term stable use of L-hydrogels under ambient conditions as soft electrodes to fabricate soft ionotronic devices including two types of triboelectric nanogenerators (TEGs), as well as capacitive ionic skin, dielectric elastomer actuators (DEAs), and flexible electroluminescent devices demonstrating the great promise of L-hydrogels for long-term practical applications in ionotronic devices.

RESULTS

Molecular design

To mimic the roles of proteins, lipids, and NMFs in the stratum corneum of human epidermis, we chose AAC, MEA, and ES to synthesize the L-hydrogels. AAC monomers,

which play a similar role to proteins in human epidermis,³⁷ contain carboxyl groups that allow for the formation of dense arrays of hydrogen bonds between AAC chains and thus can enhance the mechanical properties of the L-hydrogels and also confer extraordinary self-healing capability to L-hydrogels. The functions of hydrophilic ES and hydrophobic MEA are like those of NMFs and lipids in the human epidermis, respectively. In addition, introducing ES can mimic the non-leakage characteristics of ions of NMFs in the stratum corneum, making the cations hard to leak and stabilizing the content of ions in the network,⁴⁰ which is important for achieving stable long-term electrical properties of hydrogels. To make L-hydrogels, first, we synthesize ES monomers using the ion-exchange method (Figure S1). As shown in Figure S2, the nuclear magnetic resonance (NMR) spectrum of the synthesized ES is consistent with that reported in the literature,³² indicating that the synthesis of ES is successful. Then, the monomers—ES, AAC, and MEA—are evenly mixed with the photoinitiator-1173 to form the precursor solution. The hydrophilic ES and the hydrophobic MEA are immiscible, but the presence of AAC promotes the mixing of MEA and ES monomers (Figure S3). The liquid precursor is poured into a mold and polymerized by exposure to UV light (UV TaoYuan, 365 nm) for 20 min. The obtained copolymer films are placed in acetone solvent for 24 h, and the acetone is then evaporated to remove all unreacted monomers (Figure S4). After storing the prepared films under ambient conditions for 24 h, we successfully synthesize the L-hydrogels. The L-hydrogels are crosslinked by hydrogen bonds between AAC chain segments as well as chemical bonds formed between MEA segments due to chain transfer reactions. According to MEA, ES, and AAC content, we name the L-hydrogels MEA_x-ES_y-AAC_z, where x:y:z represents the molar ratio between the three monomers. For example, MEA₄-ES₁-AAC₄ means that the molar ratio of the three monomers in the L-hydrogel is MEA:ES:AAC = 4:1:4. In the following, we use the MEA₄-ES₁-AAC₄ L-hydrogel for characterizations and demonstrations unless otherwise stated.

Results of Fourier transform infrared (FTIR) spectroscopy of MEA₄-ES₁-AAC₄ L-hydrogel show the vibration peak (1,573 cm⁻¹) corresponding to C=C in imidazole (Figure 1C), demonstrating that ES is successfully polymerized into the network.⁴¹ The small-angle X-ray scattering (SAXS) spectrum of the L-hydrogel indicates that phase separation takes place due to the poor compatibility of ES and MEA, and the obtained L-hydrogels are transparent (Figure 1D). We characterize the water content of L-hydrogels of different compositions by measuring the weight change of L-hydrogel samples before and after drying in an oven. All tested samples are placed in a humidity chamber at 30°C and 50% relative humidity (RH) for 24 h prior to testing to ensure that the water content of the L-hydrogels is equilibrated under ambient conditions. All L-hydrogels synthesized in this work contain water content less than 12 wt % under ambient conditions (Figure 1E; Figure S5), similar to the water content of human epidermal stratum corneum and far lower than the water content of ordinary hydrogels, which is typically greater than 80 wt %. We also investigate the effect of ES, AAC, and MEA contents on the water content of L-hydrogels. With increasing ES, the equilibrium water content of L-hydrogels under ambient conditions increases from 5.5 to 9.7 wt % as the y value of MEA₄-ES_y-AAC₄ rises from 1 to 4 (Figure 1E). Although AAC also has hydrophilic carboxyl groups, its influence on the hygroscopicity of L-hydrogels is trivial since the increase of AAC has little effect on the water content of L-hydrogels (Figure S5A). On the contrary, the rise in MEA content greatly reduces the equilibrium water content of L-hydrogels under ambient conditions (Figure S5B). The results can be understood as follows: ES is a strongly hygroscopic monomer that absorbs moisture from the air—much like the NMF of human epidermis³⁸—such that the higher the content of ES, the higher the water content of L-hydrogels. Like the lipids in the human epidermis, the MEA monomer is hydrophobic, so the increase in MEA content decreases the water content of

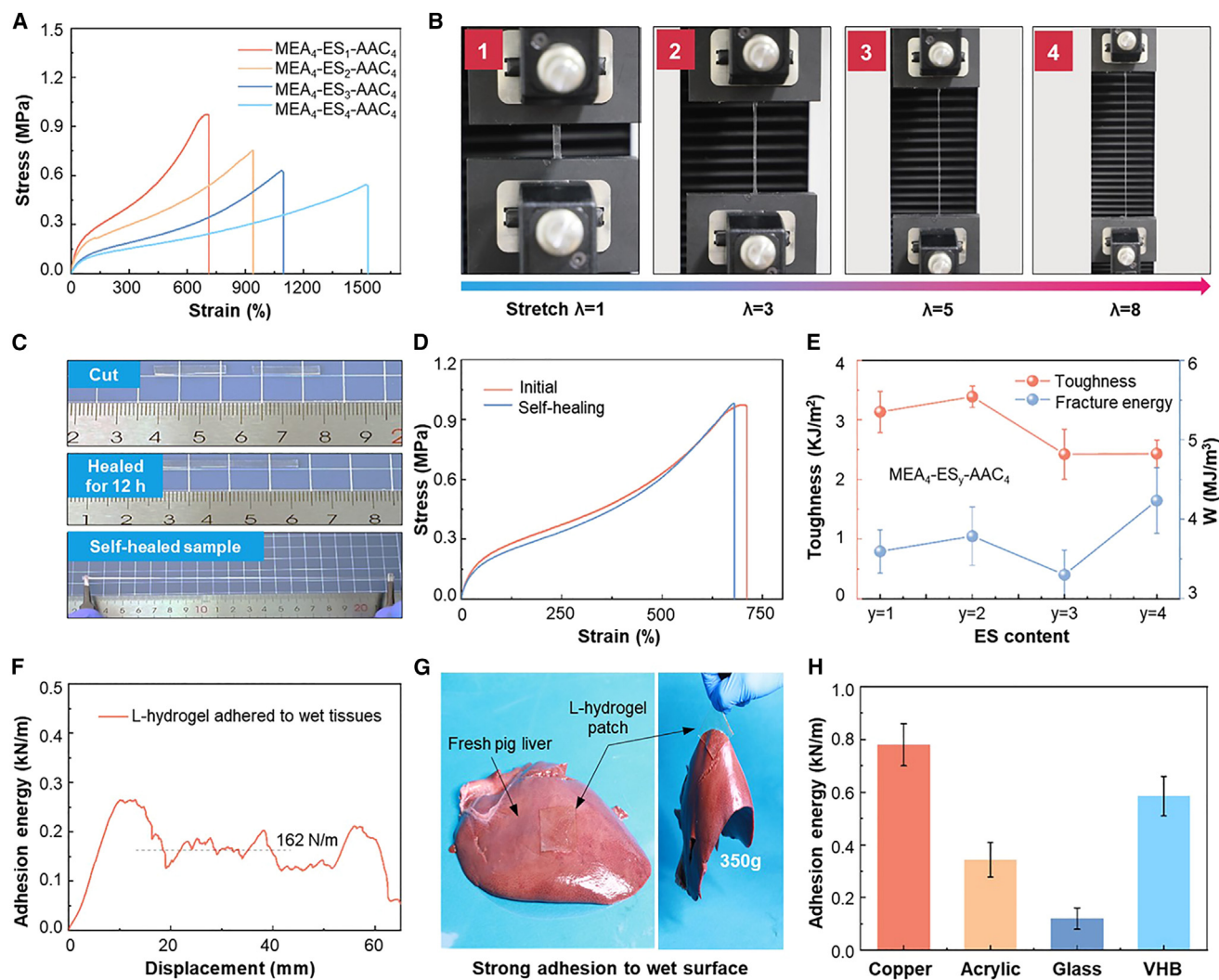


Figure 2. Enhanced mechanical properties of L-hydrogels due to low water content

(A) Stress-strain curves of L-hydrogels of different compositions (ES content). The strength of L-hydrogels can reach ~ 0.98 MPa.
 (B) Photographs of L-hydrogels subject to uniaxial tension. The sample is stretched to 8 times its original length without rupture, demonstrating sufficient stretchability.
 (C) Photographs that demonstrate the self-healing process of L-hydrogels.
 (D) Stress-strain curves of an L-hydrogel before and after 12 h self-healing. The two curves almost overlap, indicating that the healing efficiency is close to 100% according to the recovery of strength.
 (E) Fracture toughness and work of fracture of L-hydrogels with different ES content. Error bars represent the standard deviation.
 (F) Results of 90° peeling tests of L-hydrogels adhered to a typical wet biological tissue—a fresh pig liver.
 (G) Photos showing the strong adhesion of L-hydrogels to a fresh pig liver.
 (H) Adhesion energy of L-hydrogels adhered to various dry materials. The results demonstrate that L-hydrogels can achieve good adhesion to a variety of materials, from wet to dry and from soft to hard. Error bars represent the standard deviation.

L-hydrogels. This mechanism provides a route to fine-tune the water content of L-hydrogels by varying the content of MEA and ES.

Enhanced mechanical properties of L-hydrogels

Due to the low water content resulting from the integrated hydrophobic/hydrophilic design, the L-hydrogels exhibit high tensile strength and modulus under ambient conditions. Take $\text{MEA}_4\text{-ES}_1\text{-AAC}_4$ as an example: the tensile strength and modulus of the hydrogel are 0.98 and 0.93 MPa (Figure 2A; Figure S6), respectively, which

exceed those of many double-network hydrogels.^{42,43} The high tensile strength and modulus result from the low water content in the L-hydrogels, which yields sufficient hydrogen bonds between AAC chain segments to enhance mechanical performances of the hydrogel. On the contrary, in ordinary hydrogels of high water content, the presence of large amounts of water molecules weakens molecular interactions between the polar groups of hydrophilic chains, resulting in low moduli and strengths on the order of kPa.^{44,45} We provide microscopic evidence through FTIR that low water content helps to improve the mechanical properties of hydrogels. We synthesized two kinds of hydrogel, a normal low-water-content MEA₄-ES₁-AAC₄ hydrogel (L-hydrogel) and a 40%-water-content MEA₄-ES₁-AAC₄ hydrogel obtained by adding excessive water in the synthesis process. Then, we conducted FTIR tests on both hydrogels. As shown in Figure S7, the carbonyl stretching vibration peak in the FTIR of the 40%-water-content MEA₄-ES₁-AAC₄ hydrogel is at 1,720 cm⁻¹, while the carbonyl stretching vibration peak of the normal L-hydrogel is at 1,715 cm⁻¹. That is, as the water content of the hydrogel decreases, the carbonyl peak on the polymer chain shifts from 1,720 to 1,715 cm⁻¹. Such shift indicates that more carbonyls on the polymer chain form hydrogen bonds because the formation of hydrogen bonds not only averages the electron cloud of chemical bonds but also increases the bond length of C=O, and the stretching vibration of chemical bonds is inversely proportional to the square root of the bond length. The FTIR results show that when the water content is low, hydrogen bonds are easier to form between polymer chains, thus enhancing the mechanical properties of the hydrogel. Moreover, the existence of the small amount of water in the L-hydrogels also avoids significant increase in chain stiffness caused by the formation of excessive hydrogen bonds, thereby maintaining the excellent stretchability of L-hydrogels. The L-hydrogel MEA₄-ES₁-AAC₄ can be readily stretched to ~8 times its original length (Figures 2A and 2B)—a stretchability that can meet the requirements of most practical applications for soft ionotronic devices. That is, L-hydrogels can simultaneously attain high strength and stretchability thanks to the proper water content and moderate hydrogen bonds between polymer chains.

The strength and stretchability of L-hydrogels can be engineered by tuning their compositions. With the increase of ES content, the tensile strength of the L-hydrogel decreases from 0.98 to 0.54 MPa, while the strain at break increases from 709% to 1,532% (Figure 2A). In the meantime, the modulus of the gel also decreases from 0.93 to 0.25 MPa (Figure S6). This is because with increasing ES content, the water content, which acts as a plasticizer, in the hydrogel increases, reducing the strength and modulus of the material and increasing the strain at break. Moreover, the increase in AAC content increases the number of hydrogen bonds in L-hydrogels and thus enhances their tensile strength and modulus (Figure S8). In this regard, AAC in L-hydrogels plays a role similar to that of proteins in the human epidermal stratum corneum in that the presence of proteins enhances the strength and toughness of the human epidermis.³⁷ Introducing MEA as a flexible segment in the network reduces the interchain frictions and imparts good stretchability to the L-hydrogels. In comparison, hydrogels homopolymerized by ES without MEA and AAC exhibit a strength of 40 kPa and stretchability of only 30% (Figure S9), much lower than those of MEA_x-ES_y-AAC_z L-hydrogels, indicating that AAC and MEA are key to the excellent mechanical properties of L-hydrogels.

The wound-healing capability is critical to maintaining the barrier function of human skin along with preserving all other skin functions. The low-water-content strategy also imparts extraordinary self-healing capability to L-hydrogels. After cutting the sample into two separate pieces and bringing them back into contact gently (Figure 2C), polymer chains can flexibly diffuse through the interface and form hydrogen bonds

and entanglements with the network on the other side, thereby mechanically healing the cut sample under ambient conditions (Video S1). The stress-strain curves of L-hydrogels before and after the 12 h self-healing almost overlap (Figure 2D). The self-healing efficiency of L-hydrogel can reach $\sim 100\%$ based on the recovery of tensile strength and 95.36% depending on the recovery of critical strain at break. It is noteworthy that when some self-healed samples are restretched, tensile fracture even does not occur at the healed region (i.e., the original fracture site) (Figure S10), indicating a surprisingly good self-healing efficiency. The excellent self-healing ability of L-hydrogels arises from the diffusion of polymer chains through the cut interface and the subsequent formation of sufficient hydrogen bonds between AAC segments. It again indicates that AAC in L-hydrogels plays a role similar to that of proteins in the human epidermal stratum corneum since they confer self-healing capability to L-hydrogels and epidermal stratum corneum, respectively. Note that if the material contains high content of water, polymer chains that penetrate through the interface cannot form sufficient hydrogen bonds with the network in the other matrix, resulting in low self-healing efficiency. If the gel is sufficiently dried out of water, the material becomes too stiff, which significantly reduces the mobility of polymer chains and lowers the self-healing efficiency. The L-hydrogels with proper low water content can overcome these issues and attain self-healing with an efficiency of up to 100%.

The low-water-content strategy endows L-hydrogels with human-skin-like fracture toughness and work of fracture—which are measured by testing specimens with and without a notch, respectively. The fracture toughness of L-hydrogel is between 2.24 and 3.39 kJ/m² for various ES content (Figure 2E), and the work of fracture is between 3.30 and 4.23 MJ/m³. Generally, fracture toughness of traditional single-network hydrogels is usually on the order of 100 J/m².^{46,47} Compared to conventional hydrogels with high water content, the low-water-content strategy dramatically enhances the fracture resistance of L-hydrogels by increasing chain densities as well as chain interactions. In addition, due to the low water content, the friction between polymer chains becomes significant, rendering the mechanical behavior of L-hydrogels dependent on the strain rate (Figure S11): the faster the strain rate, the higher the strength and modulus of the hydrogel and the smaller the elongation at break.

The L-hydrogels can achieve strong adhesion to a wide variety of materials—from wet to dry and from soft to hard. It is well known that the adhesion of hydrogels to wet biological tissues is challenging. Although polar groups on the hydrogel surface can form physical bonds with amino, carboxyl, and hydroxyl groups on the surface of biological tissues, water on the surface of wet biological tissues separates molecules of the two surfaces, preventing the formation of strong adhesion. Intriguingly, L-hydrogels show excellent adhesion to wet biological tissues, with an adhesion energy of 162 N/m to fresh pig livers (Figures 2F and 2G). This is because L-hydrogels contain low water content under ambient conditions, so they have remarkable water absorption capability in the presence of environmental water (Figure S12) and can rapidly absorb interfacial water from the tissue surface and quickly form hydrogen bonds with polar groups on biological surfaces, thus achieving tough adhesion with tissues. Moreover, strong adhesion can be achieved simply by attaching L-hydrogels to the surface of various materials—no special adhesion methods or interfacial treatments are required—including copper, acrylic plate, glass, and VHB, with adhesion energies up to 780, 343, 120, and 585 J/m², respectively (Figure 2H; Figures S13A and S13B). The values are much higher than the natural adhesion of ordinary high-water-content hydrogels to these materials, which are typically on the order of 10 J/m². For example, the adhesion energy of polyacrylamide (PAAm) hydrogels to VHB is only 32.5 J/m², while that of L-hydrogels to VHB is

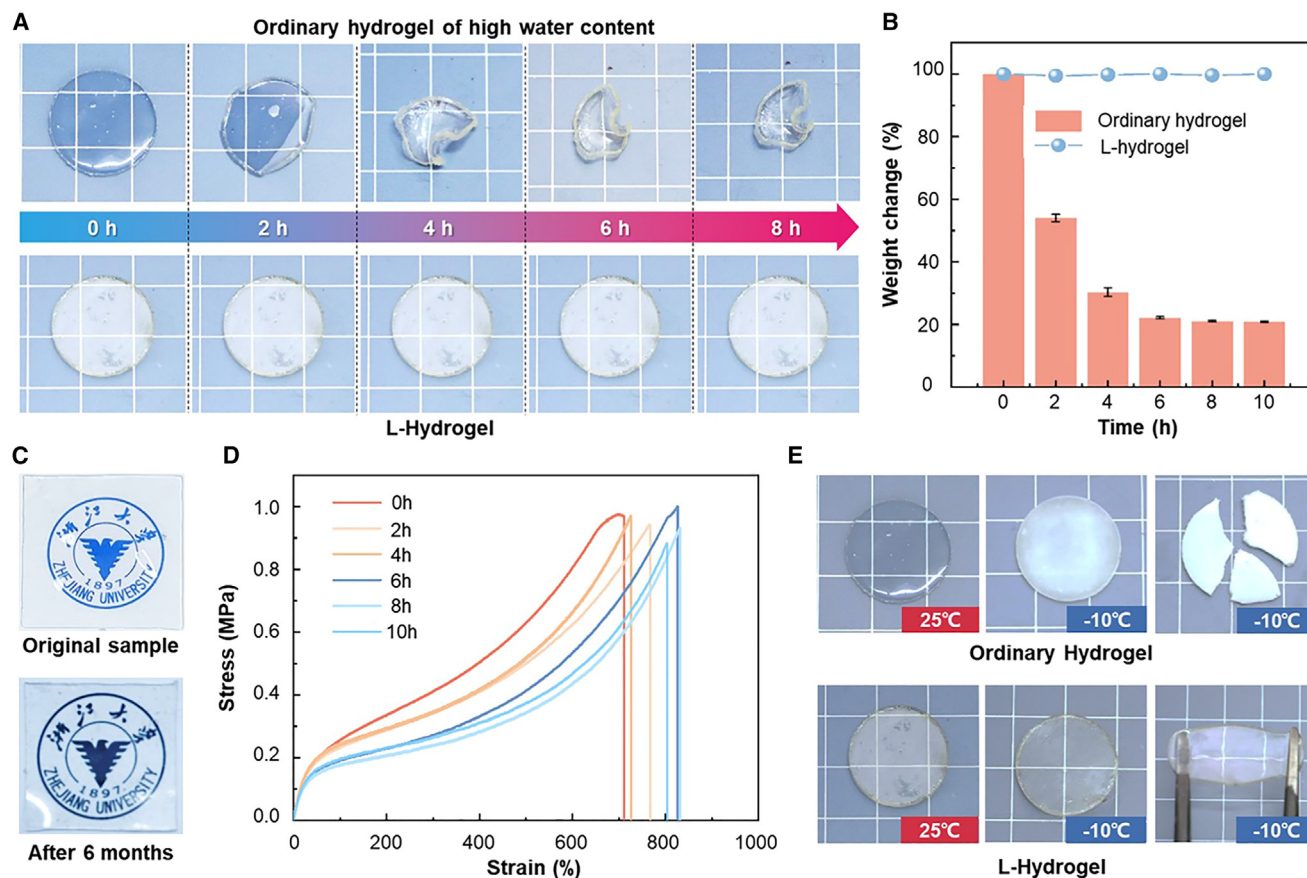


Figure 3. Stability and weather resistance of L-hydrogels

(A) Photographs of ordinary high-water-content hydrogel (i.e., PAAm hydrogel) and L-hydrogel stored under ambient conditions for 8 h. The shape and size of the PAAm hydrogel change significantly due to the rapid dehydration, whereas the change of the L-hydrogel is negligible. (B) Weight changes of L-hydrogel and PAAm hydrogel during 8 h storage under ambient conditions. The weight of PAAm hydrogel drops rapidly to 21% its original weight, while the weight change of L-hydrogel is trivial. Error bars represent the standard deviation. (C) Photos of an L-hydrogel film before and after being stored in open air for 6 months. (D) Stress-strain curves of L-hydrogels stored under ambient conditions for 10 h. (E) Photos of ordinary PAAm hydrogel and L-hydrogel stored at a low temperature of -10°C . The PAAm hydrogel freezes rapidly at -10°C and breaks easily when deformed, while the L-hydrogel can remain elastic, soft, and stretchable under -10°C .

585 J/m^2 (Figure S13C). This is because the low water content leads to a higher density of polar groups on hydrogel surfaces and fewer water molecules interfering with molecular interactions on the interface, resulting in stronger adhesion.

Stability and weather resistance of the L-hydrogels

Ordinary hydrogels of high water content are plagued by water-loss issues under ambient conditions due to the volatile nature of water. We use a typical high-water-content hydrogel, i.e., PAAm hydrogels with a water content of $\sim 80\text{ wt}\%$, as an example. Due to the evaporation of water, the shape of the PAAm hydrogel changes dramatically during 8 h storage under ambient conditions (Figure 3A), and the weight of the PAAm hydrogel drops by approximately 80% (Figure 3B), leading to a sharp reduction in stretchability from about 1,500% to 5% and an undesirable increase in modulus by roughly two orders of magnitude (Figure S14). In contrast, the L-hydrogels are quite stable under ambient conditions. The shape and weight of the L-hydrogel remain almost unchanged under ambient conditions for the same test period of 8 h (Figures 3A and 3B). After 180 days storage in an

open environment, no noticeable change of L-hydrogels could be observed (Figure 3C). Furthermore, Figure 3D shows little change in the stress-strain curves of the L-hydrogel during the storage in open environments for 8 h, which contrasts with the sharp deterioration of the mechanical properties of PAAm hydrogels under the same conditions (Figure S14). The small variation with time of the stress-strain curves of L-hydrogels mainly arises from the fluctuations in RH. To further eliminate the influence of RH variations, we place L-hydrogels in a humidity chamber at 30°C and 50% RH. The tensile stress-strain curve of the L-hydrogel after 1 month is almost identical to the original curve (Figure S15). We provide microscopic evidence through FTIR that low water content helps to improve the stability of hydrogels. We placed the prepared L-hydrogel in air for 14 days. According to Figure S7, we can find that even if L-hydrogels are placed for 14 days under ambient conditions, the stretching vibration peak of their carbonyl groups change negligibly (comparison between red and blue lines in Figure S7), which means that the number of hydrogen bonds in the hydrogel is relatively stable, so the mechanical properties of the hydrogel show good stability.

Even when L-hydrogels are dried under extremely harsh conditions—such as vacuum drying and completely dry environments (e.g., nitrogen-filled glove box), which causes the dehydration and hardening of L-hydrogels—the L-hydrogels can rapidly recover to their original water content and mechanical properties within 2 h as long as they are brought back to ambient conditions (Figure S16). Similar to the human skin,³⁴ the water content of L-hydrogels is also affected by environmental humidity. For example, as RH increases from 30% to 90%, the equilibrium water content of the MEA₄-ES₁-AAC₄ L-hydrogel in open air increases from 2.05 to 19.87 wt % (Figure S17). Although the change in water content causes the fluctuation of the mechanical properties of L-hydrogel, it is noteworthy that the L-hydrogel remains stretchable and soft with stretchability >500%, tensile strength >0.25 MPa, and modulus <2.5 MPa (Figure S18). This is significantly different from ordinary high-water-content hydrogels, which readily lose elasticity and functions in ambient air.

The low-water-content strategy also endows L-hydrogels with excellent frost resistance. We put ordinary PAAm hydrogel and L-hydrogel in an environment of −10°C for 8 h. Figure 3E shows that the PAAm hydrogel with high water content becomes white and brittle due to the freezing of internal water and loses its elasticity. In stark contrast, the L-hydrogels remain transparent and stretchable at low temperatures of −10°C. This is because the L-hydrogel contains limited water, and the presence of polymer networks prevents the nucleation and growth of ice crystals, making L-hydrogels remain soft and flexible at low temperatures. In Table S1, L-hydrogels are compared to some representative state-of-the-art hydrogels in terms of the performance and practicability so as to highlight the advantages of the L-hydrogels. The practicability and performance of the L-hydrogel, as exemplified by its stability, strength, adhesion, frost resistance, and self-healing capability, are generally superior to other state-of-the-art hydrogels. In particular, the L-hydrogel possesses unique stability in open environments that cannot be achieved by any other state-of-the-art hydrogels.

Applications of L-hydrogels in soft ionotronic devices

Because of the incorporation of ES—which acts similarly to NMFs in epidermal stratum corneum to provide dissociated ions—the L-hydrogels contain anions anchored to polymer networks and mobile cations dispersed in the network, enabling L-hydrogels to conduct electricity. We measure the conductivity of L-hydrogels of different compositions and find that the conductivity rises with increasing ES content and decreasing AAC and MEA content, with the maximum conductivity reaching

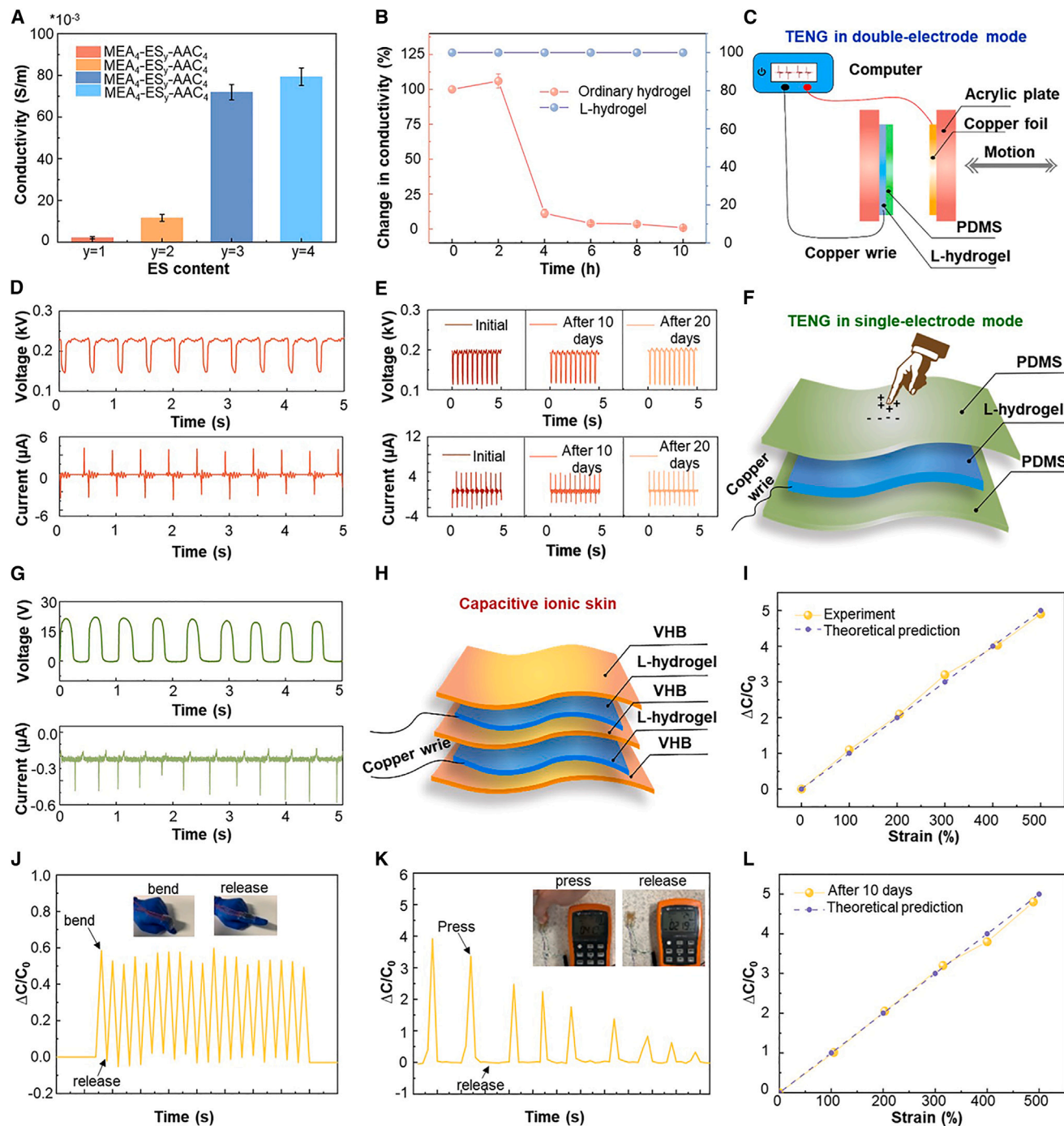


Figure 4. The application of L-hydrogels in soft ionotronic devices

(A) Conductivity of L-hydrogels with different ES content. Error bars represent the standard deviation.

(B) The conductivity change of ordinary PAAm hydrogels and L-hydrogels during 8 h storage in the open air. Error bars represent the standard deviation.

(C) Schematic diagram of L-hydrogel-based TENG in double-electrode mode.

(D) Voltage and current output signals of as-prepared L-hydrogel-based TENG tested in double-electrode mode.

(E) Voltage and current output by L-hydrogel-based TENGs after being stored under ambient conditions for 0, 10, and 20 days. Negligible changes in output signal are observed, indicating the excellent stability and durability of L-hydrogel-based TENGs.

(F) Schematic diagram of TENG in single-electrode mode.

(G) Voltage and current output by L-hydrogel-based TENG in single-electrode mode.

(H) Schematic diagram of the capacitive ionic skin.

Figure 4. Continued

(I) Capacitance of ionic skin under different strains. The capacitance change is linear with the applied strain, matching well with the theoretical predictions.

(J and K) L-hydrogel-based ionic skins working in the stretching and pressing modes, respectively.

(L) Capacitance output of L-hydrogel-based ionic skin after 10 days under ambient conditions. The response is nearly identical to that of the as-prepared ionic skin, showing the excellent stability of L-hydrogel-based ionic skin.

7.93×10^{-2} S/m (Figure 4A; Figure S19). The reason is that the increase in ES increases both the content of ions and water in L-hydrogels, which effectively improves the conductivity of L-hydrogels. Although the conductivity of L-hydrogels is lower than the value typical for high-water-content hydrogels, L-hydrogels can maintain a stable conductivity for a long time. We measure the changes in conductivity of L-hydrogels and PAAm hydrogels containing 2 M NaCl stored under ambient conditions for 8 h. The conductivity of PAAm hydrogels decreases by two to three orders of magnitude over the 8 h period, while the change in conductivity of L-hydrogels is negligible because of their relative stable water and ion content in ambient air (Figure 4B). Moreover, the anions bound in the network of L-hydrogels can attract cations through electrostatic interactions, thus avoiding ion leakage from the L-hydrogel, which mimics the non-leaking property of charged NMF in epidermal stratum corneum and contributes to the stability of conductivity of the L-hydrogels.^{32,40}

We demonstrate the applications of L-hydrogels in a series of ionotronic devices with stable performance over long periods. We first test the electrical output performance of the L-hydrogel-based TENG in the double-electrode mode. Copper foil and 184 PDMS (Polydimethylsiloxane) are employed as tribo-positive and tribo-negative materials, respectively (Figure 4C), and L-hydrogel is used as the electrode material attached to the 184 PDMS. At a frequency of 2 Hz, the TENG can steadily output a voltage of 80 V and a current of 4 μ A (Figure 4D), which can light up a blue LED bulb (Video S2). We test the changes in voltage, current, and charge of the TENGs at different frequencies (1, 1.5, 2, and 3). As the frequency increases, the voltage and charge of TENGs do not show significant changes, while the current shows a certain increase (Figure S20). Due to the stability of L-hydrogels under ambient conditions, the voltage and current signals of TENG show negligible changes after 20 day storage (Figure 4E), demonstrating the long-term stable performance of ionotronic functional devices based on L-hydrogels. Moreover, the performance of an L-hydrogel-based TENG in single-electrode model is also tested, which consists of the L-hydrogel as the electrode layer and PDMS as the electrification elastomer outer layer (Figure 4F). When touched by a finger, contact electrification generates a voltage of ~ 18 V and a current of ~ 0.4 μ A (Figure 4G), indicating that the L-hydrogels can be used in TENG-based transparent, flexible touch sensors. In addition, we also demonstrate the application of L-hydrogels in capacitive ionic skins: devices with a five-layer structure, in which VHB (Acrylate adhesive tape) is used as the dielectric layer and packaging layers, and the two L-hydrogel layers act as soft electrodes (Figure 4H). When ionic skin is laterally stretched or vertically compressed, the thickness of the dielectric layer and the area of the ionic skin change accordingly, thereby changing the capacitance of the device. It is found that the capacitance increases linearly with the applied lateral strain (Figure 4I), which agrees well with theoretical predictions.⁴⁸ Due to deformation-dependent capacitance, ionic skins based on L-hydrogels can be used to monitor the movement of human finger joints (Figure 4J). The ionic skin can also function as a pressure sensor. The higher the pressure, the more pronounced the capacitance change (Figure 4K). Again, due to the excellent stability of L-hydrogel in open environments, the performance of the ionic skin is stable in open environments over time. After 10 day storage, the capacitance-strain response of the ionic skin is nearly identical to that of the original ionic skin (Figure 4L).

We have further demonstrated the potential of L-hydrogels in electroluminescent wearable electronic devices. We prepared a dielectric layer using thermoplastic polyurethane/PMEA (Poly(2-methoxyethyl acrylate) and ZnS:Cu powder in a 1:1 mass ratio. A flexible electroluminescent bracelet is prepared by sandwiching the dielectric layer between two L-hydrogels (Figure S21B). The bracelet can emit light at 1,000 V and a 500 Hz alternating current (Figure S21B). L-hydrogels are also used to fabricate DEAs, which consist of a pre-stretched VHB layer sandwiched by two L-hydrogel films. Under 7,500 V alternating current (AC) voltage at a frequency of 0.5 Hz, the VHB layer is compressed by Maxwell force, leading to reduction in thickness and expansion in the area (as shown in Video S3). Pixel analysis shows that the area of VHB increases by 58% of its initial area under the action of voltage (Figure S22). Moreover, L-hydrogels can be employed as strain sensors due to their strain-dependent resistance (Figure S23). To this end, ionotronic devices based on L-hydrogels and their long-term stable performance demonstrate the feasibility of using L-hydrogels to construct practical ionotronic devices with excellent durability. In summary, the L-hydrogel can be used for a wide variety of applications including, but not limited to, ionic skins, TENGs, strain sensors, electroluminescent devices, strain sensors, and soft actuators.

DISCUSSION

Inspired by the low water content and stable properties of the human epidermal stratum corneum, we develop a low-water-content polyelectrolyte hydrogel (i.e., L-hydrogels) by copolymerizing AAC, hydrophobic MEA, and hydrophilic ES, which mimic the roles of proteins (strengthening and wound healing), lipids (hydrophobicity), and NMFs (hygroscopicity and ionic conductivity) in the human epidermis, respectively. The L-hydrogels can steadily maintain a low water content below 12 wt % under ambient conditions for long periods. The low water content resulting from the integrated hydrophobic/hydrophilic design leads to sufficient hydrogen bonds between AAC chain segments, giving the L-hydrogel significantly enhanced mechanical properties relative to ordinary hydrogels with high water content, including strength and modulus close to 1 MPa, self-healing capability with a healing efficiency of ~100%, and strong natural adhesion (~120–1,300 N/m) to both wet and dry surfaces. Moreover, unlike most high-water-content hydrogels that tend to lose water and function, L-hydrogels can maintain their water content stably over time under ambient conditions, giving L-hydrogels stable mechanical and electrical properties. Meanwhile, because of the low water content, the relatively dense polymer chains can inhibit the nucleation and growth of ice crystals at low temperatures, thus endowing L-hydrogels with frost resistance. We demonstrate the potential application of L-hydrogels as soft electrodes in soft ionotronics, including TENGs in different working modes and capacitive ionic skins. The performance of ionotronic devices based on L-hydrogels can remain stable for long periods. We believe that the current work provides a solution for the long-standing challenge for ordinary hydrogels: the low mechanical properties and poor stability under ambient conditions due to the high water content. Thanks to the low water content, the enhanced mechanical properties and stable material behaviors of L-hydrogels make L-hydrogels promising for practical applications in ionotronic devices that require durability and stability under ambient conditions.

EXPERIMENTAL PROCEDURES

Resource availability

Lead contact

Further information and requests for resources should be directed to and will be fulfilled by the lead contact, Zheng Jia (zheng.jia@zju.edu.cn).

Materials availability

This study did not generate new materials.

Data and code availability

The data underlying this study are available in the article and [supplemental information](#) or from the lead contact upon request.

SUPPLEMENTAL INFORMATION

Supplemental information can be found online at <https://doi.org/10.1016/j.xcrp.2023.101741>.

ACKNOWLEDGMENTS

We gratefully acknowledge the financial support from the National Key Technologies Research and Development Program (grant no. 2022YFC3203900), the Natural Science Foundation of Zhejiang Province (grant no. LR22A020005), the National Natural Science Foundation of China (grant no. 12072314), and the 111 Project (grant no. B21034).

AUTHOR CONTRIBUTIONS

Z. Shen designed the study, synthesized the samples, conducted the experiments, processed and analyzed the data, and cowrote the manuscript. Z.J. conceived the idea, supervised the project, and cowrote and revised the manuscript. All authors discussed the results.

DECLARATION OF INTERESTS

The authors declare no competing interests.

Received: June 25, 2023

Revised: October 18, 2023

Accepted: November 20, 2023

Published: December 12, 2023

REFERENCES

- Ding, B., Zeng, P., Huang, Z., Dai, L., Lan, T., Xu, H., Pan, Y., Luo, Y., Yu, Q., Cheng, H.-M., and Liu, B. (2022). A 2D material-based transparent hydrogel with engineerable interference colours. *Nat. Commun.* 13, 1212.
- He, Y., Yu, R., Li, X., Zhang, M., Zhang, Y., Yang, X., Zhao, X., and Huang, W. (2021). Digital Light Processing 4D Printing of Transparent, Strong, Highly Conductive Hydrogels. *ACS Appl. Mater. Interfaces* 13, 36286–36294.
- Yang, C., and Suo, Z. (2018). Hydrogel ionotronics. *Nat. Rev. Mater.* 3, 125–142.
- Zhang, P., Guo, W., Guo, Z.H., Ma, Y., Gao, L., Cong, Z., Zhao, X.J., Qiao, L., Pu, X., and Wang, Z.L. (2021). Dynamically Crosslinked Dry Ion-Conducting Elastomers for Soft Ionotronics. *Adv. Mater.* 33, 2101396.
- Ding, Y., Zhang, J., Chang, L., Zhang, X., Liu, H., and Jiang, L. (2017). Preparation of High-Performance Ionogels with Excellent Transparency, Good Mechanical Strength, and High Conductivity. *Adv. Mater.* 29, 1704253.
- Yu, H.C., Zheng, S.Y., Fang, L., Ying, Z., Du, M., Wang, J., Ren, K.-F., Wu, Z.L., and Zheng, Q. (2020). Reversibly Transforming a Highly Swollen Polyelectrolyte Hydrogel to an Extremely Tough One and its Application as a Tubular Grasper. *Adv. Mater.* 32, 2005171.
- Wang, Z., Zheng, X., Ouchi, T., Kouznetsova, T.B., Beech, H.K., Av-Ron, S., Matsuda, T., Bowser, B.H., Wang, S., Johnson, J.A., et al. (2021). Toughening hydrogels through force-triggered chemical reactions that lengthen polymer strands. *Science* 374, 193–196.
- Liu, C., Morimoto, N., Jiang, L., Kawahara, S., Noritomi, T., Yokoyama, H., Mayumi, K., and Ito, K. (2021). Tough hydrogels with rapid self-reinforcement. *Science* 372, 1078–1081.
- Zhao, X., Yang, J., Liu, Y., Gao, J., Wang, K., and Liu, W. (2021). An injectable and antifouling self-fused supramolecular hydrogel for preventing postoperative and recurrent adhesions. *Chem. Eng. J.* 404, 127096.
- Liang, Q., Gao, F., Zeng, Z., Yang, J., Wu, M., Gao, C., Cheng, D., Pan, H., Liu, W., and Ruan, C. (2020). Coaxial Scale-Up Printing of Diameter-Tunable Biohybrid Hydrogel Microtubes with High Strength, Perfusability, and Endothelialization. *Adv. Funct. Mater.* 30, 2001485.
- Liu, B., Xu, Z., Gao, H., Fan, C., Ma, G., Zhang, D., Xiao, M., Zhang, B., Yang, Y., Cui, C., et al. (2020). Stiffness Self-Tuned Shape Memory Hydrogels for Embolization of Aneurysms. *Adv. Funct. Mater.* 30, 1910197.
- Sun, G., Wang, P., Jiang, Y., Sun, H., Meng, C., and Guo, S. (2022). Recent advances in flexible and soft gel-based pressure sensors. *Soft Sci.* 2, 17.
- Fan, X., Chen, Z., Sun, H., Zeng, S., Liu, R., and Tian, Y. (2022). Polyelectrolyte-based conductive hydrogels: from theory to applications. *Soft Sci.* 2, 10.
- Zhao, H., Liu, M., Zhang, Y., Yin, J., and Pei, R. (2020). Nanocomposite hydrogels for tissue engineering applications. *Nanoscale* 12, 14976–14995.
- Yi, Y., Xie, C., Liu, J., Zheng, Y., Wang, J., and Lu, X. (2021). Self-adhesive hydrogels for

- tissue engineering. *J. Mater. Chem. B* **9**, 8739–8767.
16. Lee, Y., Song, W.J., and Sun, J.Y. (2020). Hydrogel soft robotics. *Materials Today Physics* **15**, 100258.
17. Huang, J., Liu, Y., Yang, Y., Zhou, Z., Mao, J., Wu, T., Liu, J., Cai, Q., Peng, C., Xu, Y., et al. (2021). Electrically programmable adhesive hydrogels for climbing robots. *Sci. Robot.* **6**, eabe1858.
18. Cao, Y., Morrissey, T.G., Acome, E., Allec, S.I., Wong, B.M., Keplinger, C., and Wang, C. (2017). A Transparent, Self-Healing, Highly Stretchable Ionic Conductor. *Adv. Mater.* **29**, 1605099.
19. Mandal, S., Kumari, S., Kumar, M., and Ojha, U. (2021). Supplementary Networking of Interpenetrating Polymer System (SNIPs) Strategy to Develop Strong & High Water Content Ionic Hydrogels for Solid Electrolyte Applications. *Adv. Funct. Mater.* **31**, 2100251.
20. Liu, J., Chen, Z., Chen, Y., Rehman, H.U., Guo, Y., Li, H., and Liu, H. (2021). Ionic Conductive Organohydrogels with Dynamic Pattern Behavior and Multi-Environmental Stability. *Adv. Funct. Mater.* **31**, 2101464.
21. Li, X., Lou, D., Wang, H., Sun, X., Li, J., and Liu, Y.-N. (2020). Flexible Supercapacitor Based on Organohydrogel Electrolyte with Long-Term Anti-Freezing and Anti-Drying Property. *Adv. Funct. Mater.* **30**, 2007291.
22. Zhang, X.-F., Ma, X., Hou, T., Guo, K., Yin, J., Wang, Z., Shu, L., He, M., and Yao, J. (2019). Inorganic Salts Induce Thermally Reversible and Anti-Freezing Cellulose Hydrogels. *Angew. Chem. Int. Ed.* **58**, 7366–7370.
23. Yuk, H., Zhang, T., Parada, G.A., Liu, X., and Zhao, X. (2016). Skin-inspired hydrogel–elastomer hybrids with robust interfaces and functional microstructures. *Nat. Commun.* **7**, 12028.
24. Zhu, T., Jiang, C., Wang, M., Zhu, C., Zhao, N., and Xu, J. (2021). Skin-Inspired Double-Hydrophobic-Coating Encapsulated Hydrogels with Enhanced Water Retention Capacity. *Adv. Funct. Mater.* **31**, 2102433.
25. Xu, Z., Zhou, F., Yan, H., Gao, G., Li, H., Li, R., and Chen, T. (2021). Anti-freezing organohydrogel triboelectric nanogenerator toward highly efficient and flexible human-machine interaction at -30°C . *Nano Energy* **90**, 106614.
26. Liu, Y., Li, H., Wang, X., Lv, T., Dong, K., Chen, Z., Yang, Y., Cao, S., and Chen, T. (2021). Flexible supercapacitors with high capacitance retention at temperatures from -20 to 100°C based on DMSO-doped polymer hydrogel electrolytes. *J. Mater. Chem. A* **9**, 12051–12059.
27. Jian, Y., Handschuh-Wang, S., Zhang, J., Lu, W., Zhou, X., and Chen, T. (2021). Biomimetic anti-freezing polymeric hydrogels: keeping soft-wet materials active in cold environments. *Mater. Horiz.* **8**, 351–369.
28. Manish, V., Arockiarajan, A., and Tamadapu, G. (2021). Influence of water content on the mechanical behavior of gelatin based hydrogels: Synthesis, characterization, and modeling. *Int. J. Solid Struct.* **233**, 111219.
29. Li, Z., Liu, Z., Ng, T.Y., and Sharma, P. (2020). The effect of water content on the elastic modulus and fracture energy of hydrogel. *Extreme Mechanics Letters* **35**, 100617.
30. Zhou, Z., Lei, J., and Liu, Z. (2022). Effect of water content on physical adhesion of polyacrylamide hydrogels. *Polymer* **246**, 124730.
31. Osaki, M., Yonei, S., Ueda, C., Ikura, R., Park, J., Yamaguchi, H., Harada, A., Tanaka, M., and Takashima, Y. (2021). Mechanical Properties with Respect to Water Content of Host–Guest Hydrogels. *Macromolecules* **54**, 8067–8076.
32. Kim, H.J., Chen, B., Suo, Z., and Hayward, R.C. (2020). Ionoelastomer junctions between polymer networks of fixed anions and cations. *Science* **367**, 773–776.
33. Spencer, T.S., Linamen, C.E., Akers, W.A., and Jones, H.E. (1975). Temperature dependence of water content of stratum corneum. *Br. J. Dermatol.* **93**, 159–164.
34. Galliano, M.-F., Tfayli, A., Dauskardt, R.H., Payre, B., Carrasco, C., Bessou-Touya, S., Baille-Guffroy, A., and Duplan, H. (2021). Comprehensive characterization of the structure and properties of human stratum corneum relating to barrier function and skin hydration: modulation by a moisturizer formulation. *Exp. Dermatol.* **30**, 1352–1357.
35. Boireau-Adamezyk, E., Baille-Guffroy, A., and Stamatias, G.N. (2021). The stratum corneum water content and natural moisturization factor composition evolve with age and depend on body site. *Int. J. Dermatol.* **60**, 834–839.
36. Yamada, T., Habuka, A., and Hatta, I. (2021). Moisturizing mechanism of glycerol and diglycerol on human stratum corneum studied by synchrotron X-ray diffraction. *Int. J. Cosmet. Sci.* **43**, 38–47.
37. Bissett, D.L., McBride, J.F., and Patrick, L.F. (1987). Role of protein and calcium in stratum corneum cell cohesion. *Arch. Dermatol. Res.* **279**, 184–189.
38. Hoffman, D.R., Kroll, L.M., Basehoar, A., Reece, B., Cunningham, C.T., and Koenig, D.W. (2015). Immediate and extended effects of abrasion on stratum corneum natural moisturizing factor. *Skin Res. Technol.* **21**, 366–372.
39. Murata, T., Honda, T., Mostafa, A., and Kabashima, K. (2022). Stratum corneum as polymer sheet: concept and cornification processes. *Trends Mol. Med.* **28**, 350–359.
40. Lee, C.-J., Wu, H., Hu, Y., Young, M., Wang, H., Lynch, D., Xu, F., Cong, H., and Cheng, G. (2018). Ionic Conductivity of Polyelectrolyte Hydrogels. *ACS Appl. Mater. Interfaces* **10**, 5845–5852.
41. Berdzinski, S., Strehmel, B., and Strehmel, V. (2015). Photogenerated lophyl radicals in 1-alkyl-3-vinylimidazolium bis(trifluoromethylsulfonyl)imides. *Photochem. Photobiol. Sci.* **14**, 714–725.
42. Xu, X., Jerca, V.V., and Hoogenboom, R. (2021). Bioinspired double network hydrogels: from covalent double network hydrogels via hybrid double network hydrogels to physical double network hydrogels. *Mater. Horiz.* **8**, 1173–1188.
43. Li, L., Wu, P., Yu, F., and Ma, J. (2022). Double network hydrogels for energy/environmental applications: challenges and opportunities. *J. Mater. Chem. A* **10**, 9215–9247.
44. Tan, M., Zhao, T., Huang, H., and Guo, M. (2013). Highly stretchable and resilient hydrogels from the copolymerization of acrylamide and a polymerizable macromolecular surfactant. *Polym. Chem.* **4**, 5570–5576.
45. Xue, S., Pei, D., Jiang, W., Mu, Y., and Wan, X. (2016). A simple and fast formation of biodegradable poly(urethane-urea) hydrogel with high water content and good mechanical property. *Polymer* **99**, 340–348.
46. Zhao, X. (2017). Designing toughness and strength for soft materials. *Proc. Natl. Acad. Sci. USA* **114**, 8138–8140.
47. Yang, J., Li, K., Tang, C., Liu, Z., Fan, J., Qin, G., Cui, W., Zhu, L., and Chen, Q. (2022). Recent Progress in Double Network Elastomers: One Plus One is Greater Than Two. *Adv. Funct. Mater.* **32**, 2110244.
48. Sun, J.-Y., Keplinger, C., Whitesides, G.M., and Suo, Z. (2014). Ionic skin. *Adv. Mater.* **26**, 7608–7614.